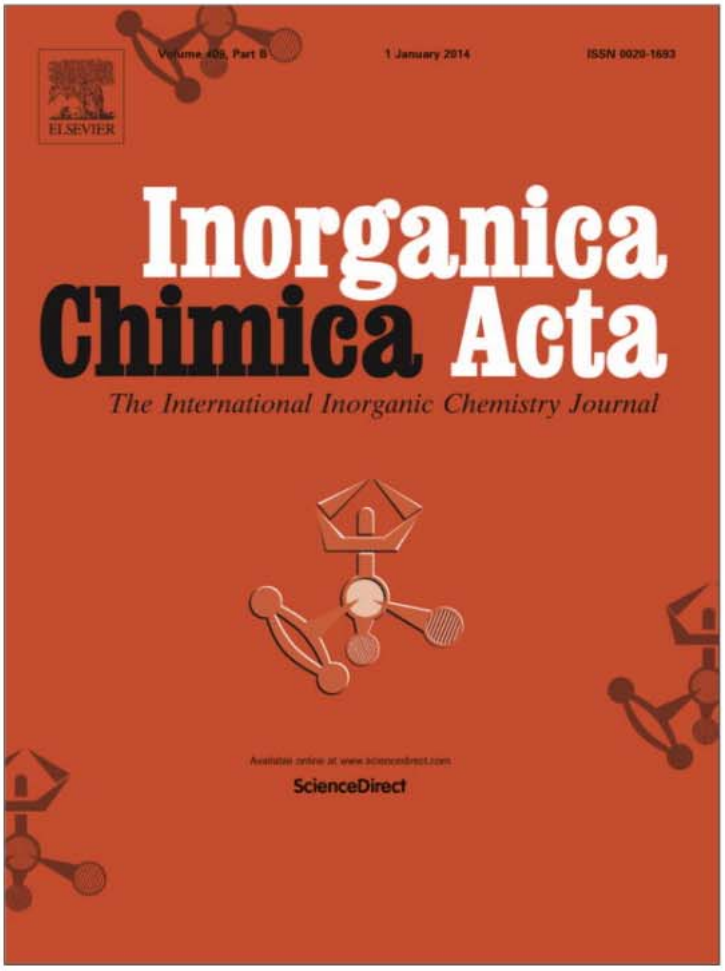

Inorganica Chimica Acta 409 (2014) 342–348

Contents lists available at ScienceDirect

Inorganica Chimica Acta

journal homepage: www.elsevier.com/locate/ica

Photochemistry of supramolecular complex formed by *trans*-stilbene and the metal–organic coordination polymer

Veronica V. Semionova [a], Evgeni M. Glebov [a,b,*], Valeri V. Korolev [a], Sergey A. Sapchenko [c], Denis G. Samsonenko [c,b], Vladimir P. Fedin [c,b]

[a] Voevodsky Institute of Chemical Kinetics and Combustion, Novosibirsk 630090, Russia
[b] Novosibirsk State University, Novosibirsk 630090, Russia
[c] Nikolaev Institute of Inorganic Chemistry, Novosibirsk 630090, Russia

ARTICLE INFO

Article history:
Received 16 July 2013
Received in revised form 19 September 2013
Accepted 27 September 2013
Available online 8 October 2013

Keywords:
Metal–organic frameworks
Organic photochroms
Supramolecular adducts
Photochemistry
Photochromism

ABSTRACT

Supramolecular adduct consisting from the metal–organic framework (MOF) $[Zn_4(dmf)(ur)_2(ndc)_4]$ (ndc^{2-} is 2,6-naphtalenedicarboxylate, ur is urotropin, and dmf is *N*,*N*′-dimethylformamide) and *trans*-stilbene was synthesized and its photochemistry was studied. The quantum yield of *trans*–*cis* photoisomerization of stilbene in adduct (0.2) was found to be an order of magnitude higher than for crystalline *trans*-stilbene and comparable with that in organic solvents. The results demonstrate that the creation of MOFs adducts with organic photochroms is a prospective approach for the creation of new hybrid photochromic materials.

1. Introduction

Organic photochromic compounds are prospective for the development of various photosensitive systems, such as optical media with nonlinear absorption, systems of optical information recording, and optical switchers [1,2]. Of special interest are compounds retaining photochemical activity in the crystal state [3,4]. Only a few classes of organic photochroms are active in the crystal state. This is explained by the fact that the photochromic reaction typically needs sufficient free volume to occur. Photochromic transformations were observed both in polycrystalline films and in single crystals of diarylethenes [5,6], derivatives of salicylic aldehyde [4,7], arylhydrazides [8], and fulgides [9]. In all these cases large free volume is not necessary for the photochromic transformations to occur. Quite unexpected are examples of crystal state photochromism of chromenes [10], spiropyrans [11] and spirooxazines [12]. In the case of chromenes and spirocompounds the free volume necessary for photoisomerization is rather high, therefore, no photochemical activity is typically observed in the crystal state. In the mentioned examples, the free volume was provided either by cavities in the crystal packing or by large size of any functional group of the molecule [11,12].

The advantages of crystal photochroms in comparison with those dissolved in liquids or in polymers are easy handling and high fatigue resistance [4]. Increase in fatigue resistance is caused by the absence of unwanted photochemical reactions, in which solvent molecules are typically involved [13]. On the other side, the quantum yields of photochemical reactions in the solid state are usually significantly lower than in solutions [12]. This is a challenge to create a crystal photochromic material combining advantages of liquid state (high quantum yield) and crystal state (high fatigue resistance).

One of the possible approaches to solve this problem is the creation of hybrid organic-inorganic compounds [14]. Research interests in organic–inorganic hybrid photochromic materials cover a wide range. The problems can be classified into three categories (see review [15] and references there): (1) improving the photochromic behavior (quantum yield, duration, response, reversibility, sensitivity, thermal stability, and wavelength coverage of absorption or emission) of photochromophores via hybrid formation; (2) manufacturing "smart" photoresponsive systems with various switchable functions (chirality, luminescence, electric and magnetic properties, catalysis, photomechanics, release/sorption, etc.) using photochromophores; (3) exploring new families of photochromic materials with non-photochromic components. The char-

* Corresponding author at: Voevodsky Institute of Chemical Kinetics and Combustion, Novosibirsk 630090, Russia. Tel.: +7 383 3332385; fax: +7 383 3307350.
E-mail address: glebov@kinetics.nsc.ru (E.M. Glebov).

0020-1693/$ - see front matter © 2013 Elsevier B.V. All rights reserved.
http://dx.doi.org/10.1016/j.ica.2013.09.048

acteristics of photochromic hybrid materials could be superior to the characteristics of starting compounds. E.g., electron transfer between organic and inorganic parts of the hybrid materials based on transition metal oxides and polyoxometalates were reported to result in improving photochromic properties [16]. Polyoxometalates incorporated into hybrid matrices are considered as prospective systems for manufacturing of molecular optical switches and optical memory devices [17].

The approach developing in this work is to use metal-organic coordination polymers (also called metal-organic frameworks (MOF) [18]) for producing supramolecular compounds with organic photochroms. MOFs are crystalline compounds comprising metal ions (or clusters, or polynuclear fragments) coordinated to electrically neutral or negatively charged bridging organic ligands to form one-, two- or three-dimensional structures. MOFs are widely used for synthesis of host-guest inclusion compounds [18]. We believe that the incorporation of an organic photochromic compound into a MOF can result in creation of photochromic material with high resistance to photodegradation and high quantum yields. To our knowledge, compounds like that were not reported in literature.

For preliminary experiments, a recently reported [19] metal–organic coordination polymer $Zn_4(dmf)(ur)_2(ndc)_4$, where ndc^2 is 2,6-naphtalenedicarboxylate, ur is urotropin, and dmf is *N,N′*-dimethylformamide (Fig. 1) and a well-known organic photochrom stilbene (Scheme 1) were chosen. Stilbenes were used to study their phototransformations on flat surfaces [20], in zeolites [21], crystalline cyclodextrin inclusion complexes [22] and calixarenes van der Waals nanocapsules [23]. For reference, Fig. 2 shows UV absorption and luminescence spectra of *trans*- and *cis*-stilbene in acetonitrile solutions. The size of the MOF channels is 10.5 × 10.5 Å, and it fits well to stilbene. In this work, the adduct of the MOF with stilbene was synthesized, and its photochemistry was studied.

2. Experimental

2.1. Reagents and materials

Trans- and *cis*-stilbene (Aldrich) were used without additional purification. Samples for *cis*-stilbene photolysis in aqueous solutions ere prepared as described in [24]. Synthesis and physical properties of the metal-organic coordination polymer $[Zn_4(dmf)(ur)_2(ndc)_4]$ (further referred as MOF-1) were described in [19]. Its molecular formula is $C_{63}H_{55}N_9O_{17}Zn_4$. Liquid phase experiments were performed with high purity grade acetonitrile ("Kriokhrom", Russia) as a solvent. FT-IR grade KBr (Aldrich) was used for preparation of pellets for solid state experiments. In several experiments, porous glass plates PS-2 (Vavilov State Optical Institute, Russia) with average pore size 7 nm [25] were used as supports for organic photochroms.

2.2. Synthesis of MOF-1 adduct with trans-stilbene

Supramolecular compound of MOF-1 ($C_{63}H_{55}N_9O_{17}Zn_4$) and *trans*-stilbene ($C_{14}H_{12}$) is further referred as Adduct-1. MOF-1 (0.1 g) and *trans*-stilbene in 10-fold excess (0.13 g) were placed into an ampoule, evacuated and heated to 105 °C for 24 h. Acetonitrile, in which MOF-1 was insoluble, was used for washing the adduct of the residual *trans*-stilbene. Then the formed adduct was wrung out between two sheets of filter paper and dried under air. The resulted Adduct-1 appears as pale-yellow crystals. Elemental analysis of Adduct-1 corresponds to the 3:1 ratio of *trans*-stilbene to MOF-1 suggesting the empirical formula $[Zn_4(dmf)(ur)_2(ndc)_4]\cdot 3C_{14}H_{12}$ ($C_{105}H_{91}N_9O_{17}Zn_4$). *Anal.* Calc. C, 62.7; H, 4.6; N, 6.3. Found: C, 62.4; H, 4.5; N, 6.2%. The data of elemental analysis are in a good agreement with single-crystal X-ray data (see below).

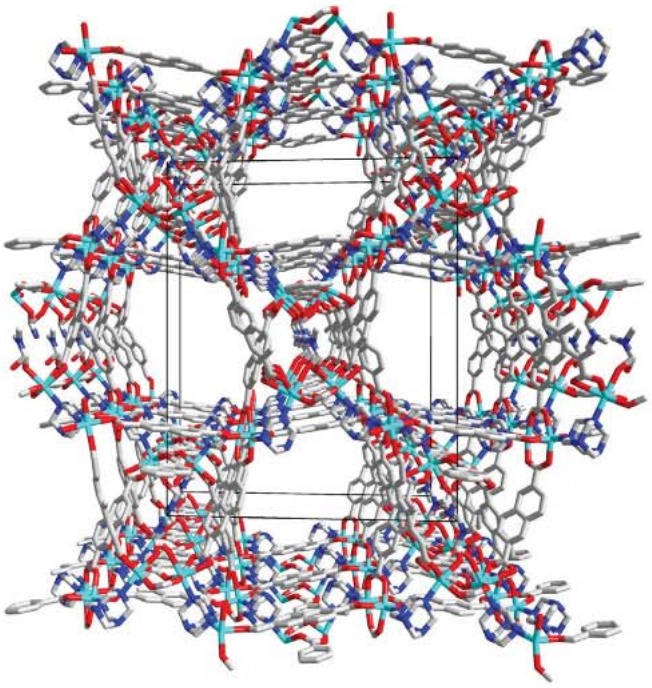

Fig. 1. Fragment of the framework MOF-1 structure (wire presentation). View along *a* axis. Hydrogen atoms are omitted for clarity.

2.3. X-ray crystallography

Single-crystal XRD data collections of Adduct-1 were performed by using an automated four circle Bruker–Nonius X8Apex CCD diffractometer with Mo-Ka radiation (λ = 0.71073 Å). Absorption correction based on the intensities of equivalent reflections was

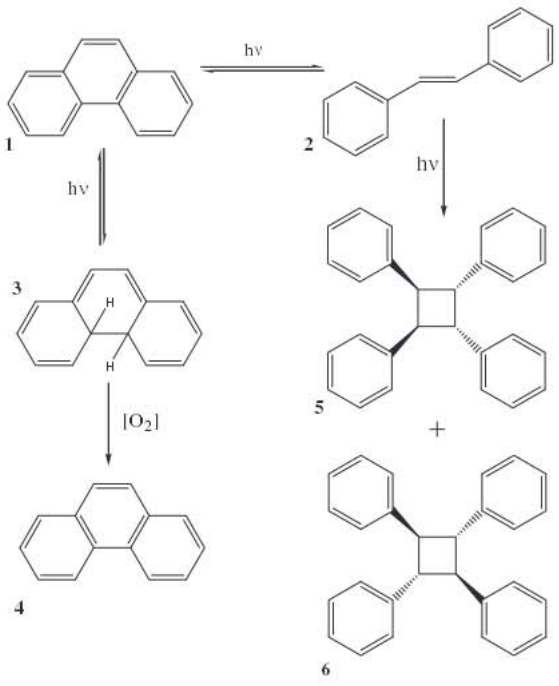

Scheme 1. Photochemical reactions of stilbenes.

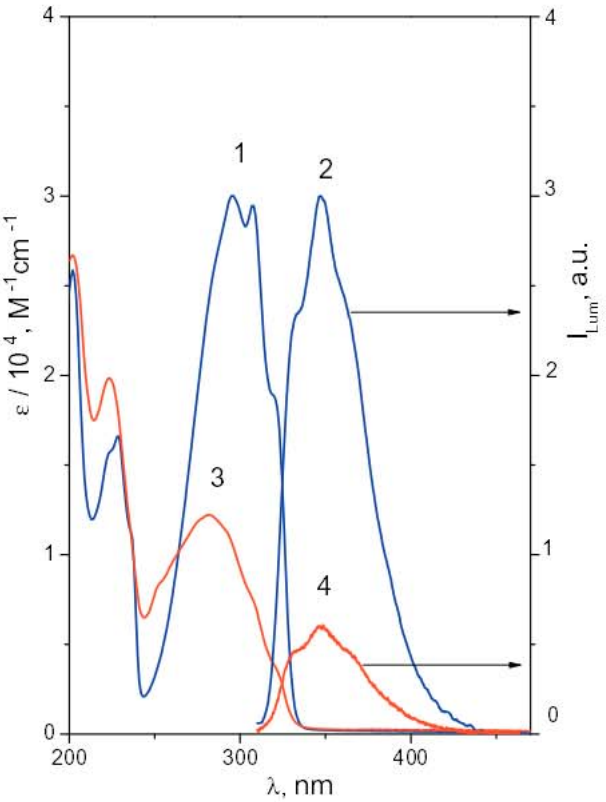

Fig. 2. Absorption and luminescence spectra of *trans*-stilbene (curves 1 and 2) and *cis*-stilbene (curves 3 and 4) in acetonitrile.

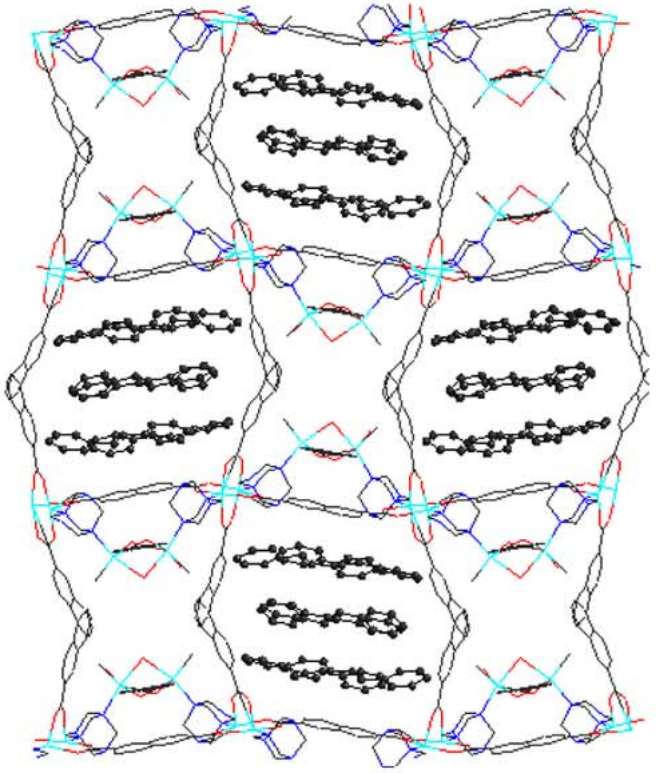

Fig. 3. Fragment of Adduct-1 structure (wire presentation). View along *a* axis. Hydrogen atoms are omitted for clarity.

performed using the SADABS program [26]. The structures were solved by direct method and refined on F^2 by full-matrix least-squares method in the anisotropic approximation (for non-hydrogen atoms) using SHELX-97 program package [27]. Positions of the hydrogen atoms of 2,6-naphtalenedicarboxylate, urotropine ligands and guest *trans*-stilbene were calculated geometrically and refined by the rigid model. Crystal data for $[Zn_4(dmf)(ur)_2(ndc)_4]\cdot 3C_{14}H_{12}$: monoclinic, P $2_1/n$, $a = 12.2950(4)$, $b = 30.7547(10)$, $c = 24.7649(9)$ Å, $\beta = 97.530(1)°$, $V = 9283.6(5)$ Å^3, $Z = 4$, $T = 100(2)$ K, $\rho_{calc} = 1.440$ g cm^{-1}, $R_1 = 0.1089$ (for reflections with $I > 2\sigma(I)$), Goodness-of-fit (GOF) on $F^2 = 1.179$. The atoms of two carboxylate groups of the ndc^{2-} moieties and coordinated dmf ligand are disordered over two half-occupied positions. The crystallographic data and details of the structure refinements are summarized in Table S1. Selected interatomic distances and valence angles are given in Table S2.

The single-crystal X-ray crystallography reveals that the framework structure in Adduct-1 is similar to starting MOF-1. The 1D channels are filled with *trans*-stilbene molecules (3 molecules per formula unit, Fig. 3). There are no special interactions either between the different guest molecules or between the guest molecules and the framework.

Absence of residual solvent (acetonitrile) in the pores of MOF-1 was supported by means of IR spectroscopy. The band of the *C—N* triple bond stretching vibration (2240–2260 cm^{-1}) did not appear in the IR spectrum of Adduct-1.

2.4. Preparation of solid samples

Two types of samples were used for recording solid-state UV absorption and luminescence spectra of *trans*-stilbene and Adduct-1. Samples of the first type were KBr pellets containing dispersed target material prepared by means of standard procedure used in the IR spectroscopy. For preparation of optically transparent pellets weighted amount of KBr was crushed in an agate mortar, dried at a temperature of 130 °C for 12 hrs and evacuated for 24 h. Then weighted amount of the target substance was finely grinded with pre-prepared KBr and pressed at 200 atm. The prepared pellets were stored in the evacuated dessicator. A typical example of the UV spectrum of a blank KBr pellet is shown in Fig. 4 (curve 1). In spite of significant light scattering, pellets were transparent enough for using in the UV spectroscopy.

Samples of the second type were prepared by the impregnation of a porous glass plate with solution of *trans*-stilbene in acetonitrile followed by evacuation. The UV spectrum of a blank porous glass is shown in Fig. 4 (curve 2). The wavelength region of $\lambda > 260$ nm is available for measurements.

2.5. Instrumental measurements

UV absorption spectra were recorded using an Agilent 8453 (Agilent Technologies) and Varian Cary 50 spectrophotometers. Luminescence spectra were recorded using a Hitachi MFP-4 spectrofluorimeter. Elemental analyses on C, H, and N were performed by means of a Euro EA 3000 CHN elemental analyzer (EuroVector Instruments). FTIR spectra (KBr pellets) were recorded in the range of 4000–400 cm^{-1} on a Scimitar FTS 2000 Fourier-transform infrared spectrometer (Digilab LLC). Powder X-ray diffraction (PXRD) data were collected with Cu Kα irradiation on a Philips PW 1830 instrument equipped with a PW 1820 vertical Bragg-Brentano powder goniometer and a PW 1710 control unit.

2.6. Photochemical experiments

Stationary photolysis was performed using a high pressure mercury lamp with sets of glass filters to select light with the necessary

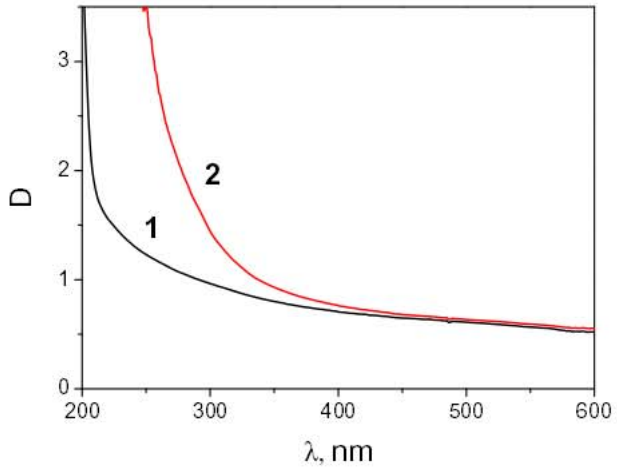

Fig. 4. UV spectra of a 0.045 cm thick KBr pellet (curve 1) and a porous glass PS-2 (curve 2).

wavelengths. Assuming homogeneous distribution of the absorbing substance in the sample, one can estimate quantum yield of the photolysis in solid samples (Eq. (1)). The characteristic feature of the samples used in this work was the significant optical density at the excitation wavelength caused by the properties of the support. The observed UV spectrum of a KBr pellet is determined by substantial light scattering, and the observed spectrum of porous glass is caused by both of scattering and absorption (Fig. 4). In this case, one has to take into account that only a part of incident light ($I^{Abs}_{Stilbene}$) is absorbed by the target substance. The correction was made using Eq. (2).

$$\varphi = \frac{\frac{dD_\lambda}{dt} \times V \times N_A}{\Delta\varepsilon_\lambda \times L \times I^{Abs}_{Stilbene}} \quad (1)$$

$$I^{Abs}_{Stilbene} = (1 - 10^{-(D_{Stilbene}+D_{Support})}) \times \frac{D_{Stilbene}}{D_{Stilbene} + D_{Support}} \quad (2)$$

Here $\frac{dD_\lambda}{dt}$ is the rate of absorption change (at the probing wavelength λ) in the course of photolysis at low conversions, V is the volume of the irradiated part of the sample; L is the sample thickness; N_A is Avogadro number; $I^{Abs}_{Stilbene}$ is the intensity of light absorbed by *trans*-stilbene, I_0 is the incident light intensity (typically 10^{15}–10^{16} quanta/s), $D_{Stilbene}$ and $D_{Support}$ are the optical densities of *trans*-stilbene and support at the excitation wavelength (313 nm in our experiments); and $\Delta\varepsilon_\lambda$ is the difference in molar absorption coefficients of initial compound and product at the probing wavelength λ. Light intensity was measured by means of SOLO 2 power and energy meter (Gentec EO). The value of $\Delta\varepsilon_\lambda$ for the solid state was taken equal to that measured in solutions. All the values of quantum yields were found by averaging on the experiments with four samples.

3. Results and discussion

3.1. Photochemical processes possible for stilbene

Photochemistry of stilbene in solutions was widely studied (see e.g. review [28] and references there). The possible photochemical reactions of *trans*- and *cis*-stilbene [23] are shown in Scheme 1. Stilbene exhibits reversible *trans–cis* photoisomerization (compounds **1** and **2** in Scheme 1), photocyclization of *cis*-stilbene to dihydrophenanthrene (**3**) followed by oxidation to phenanthrene (**4**), and Diels–Alder dimerization of *trans*-stilbene to yield tetraphenylcyclobutane products (**5** and **6**). Photoisomerization and photocyclization occur in all common organic solvents [29,30]. Unsubstituted stilbenes typically do not undergo photodimerization in organic solvents [28]. However, this reaction was observed in aqueous solutions, in which stilbene aggregates are formed starting from as low concentration as 10^{-6} M [24].

Before studying photochemistry of *trans*-stilbene in the solid state and in adduct with MOF, it was necessary to refer to the spectral changes caused by the photolysis in solutions. Fig. 5 shows the changes in the UV spectrum of *trans*-stilbene originate from its photolysis in a common organic solvent (acetonitrile). On the first stage (Fig. 5a) *trans–cis* isomerization occurs, which manifests itself as a decrease of absorption in the region 270–330 nm, and the isosbestic point at 264 nm is conserved. Another manifestation of *trans* to *cis* transition is the decrease in the intensity of luminescence (Fig. 2). Mutual *trans–cis* and *cis–trans* transitions lead to establishing of the photostationary state (equilibrium between *trans* and *cis* isomers) [30]. Prolonged irradiation results in photocyclization of *cis*-stilbene to dihydrophenanthrene followed by its oxidation to phenanthrene (Scheme 1). This process manifests itself as the appearance of characteristic spectrum of phenanthrene with the peaks at 251, 274, 281 and 293 nm (Fig. 5b).

Yet another possible reaction in stilbene photochemistry is the formation of dimers via Diels–Alder reaction (Scheme 1). In fact, this is a way to the photodegradation of photochromic system additional to the formation of phenanthrene. The photodimers were detected in the case of stilbene photolysis in aqueous solutions, but not in organic solvents [29] (it should be noted that because of very low solubility of *trans*-stilbene in water, experiments in aqueous solutions were always started with *cis*-stilbene). The formation of photodimers was also reported for *trans*-stilbene molecules incorporated into γ-cyclodextrin [22] and into nanocapsules formed by two calixarene molecules [23]. In all these cases photodimers were detected either by chromatography or by NMR. In or-

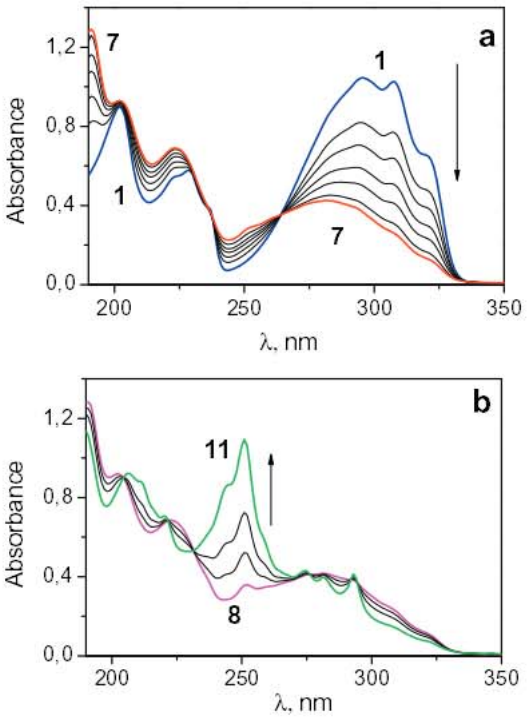

Fig. 5. Changes in the UV spectrum caused by *trans*-stilbene photolysis (313 nm) in CH_3CN. 1 cm cell, initial concentration 3.5×10^{-5} M. (a) Initial stage of photolysis interpreted as *trans–cis* isomerization. Curves 1–7 correspond to 0, 7, 13, 20, 30, 45, 70 s of irradiation. (b) Prolonged photolysis interpreted as transition of *cis*-stilbene to phenanthrene. Curves 8–11 correspond to 230, 650, 1300, 2400 s of irradiation.

der to examine the possible formation of photodimers for the case of stilbene incorporated into the MOF cage by means of UV spectroscopy, we firstly performed experiments on the prolonged photolysis of *cis*-stilbene in aqueous solutions.

Prolonged photolysis of *cis*-stilbene in water monitored by UV spectroscopy (Fig. 6) resulted in the formation a plateau in the region of 350–450 nm. For comparison, Fig. 6 demonstrates the spectra of *cis*-stilbene and phenanthrene. The plauteau was observed only in aqueous solutions, but not in organic solvents. Therefore, we conclude that the formation of a plauteau in the region of 350–450 nm is a signature of Diels–Alder photodimers (Scheme 1).

3.2. Photochemistry of stilbene in polycrystalline state

As we know, there is no information in the literature concerning the *trans*-stilbene photolysis in the crystalline state. The possible photochemical activity of samples prepared by dispersing of solid *trans*-stilbene into KBr pellets was examined by means of luminescent and UV spectroscopy. Both methods demonstrated the occurrence of a photochemical reaction. The typical results are presented in Fig. 7. Note that the initial spectrum of *trans*-stilbene luminescence (curve 1 in Fig. 7a) contains resolved peaks with the maxima at 363 and 379 nm and a shoulder in the region of 400 nm, while in the spectrum recorded in solution (curve 2 in Fig. 2) the two peaks are not resolved. Both luminescence intensity (Fig. 7a) and UV absorption (Fig. 7b) of the samples were decreased in the course of irradiation. The observed spectral changes correspond to *trans–cis* isomerization and establishing of equilibrium between *trans*- and *cis*-isomers. Spectral changes characteristic of either photocyclization or photodimerization were not observed (see Figs. 5b and 6 for comparison). Therefore, we conclude that the reaction of *trans–cis* photoisomerization is the only reaction occurring in the crystalline *trans*-stilbene.

Quantum yield of *trans–cis* photoisomerization was estimated using Eqs. (1) and (2). The values of the quantum yields for all the systems described in this work are collected in Table 1. The quantum yield of polycrystalline *trans*-stilbene photoisomerization is rather small (about two orders of magnitude lower than in solution). The decrease of quantum yield could be explained using the known reaction mechanism. Photoisomerization of stilbenes occurs via short-living 90° twisted intermediate state [31]. The attainment of the twisted state needs a sufficient free volume. In the case of crystalline *trans*-stilbene, the reaction is possible only for the molecules which are situated on the surface of small polycrystals dispersed in a KBr pellet. It is essentially to assume that the quantum yield of *trans–cis* isomerization is proportional to the number of molecules which have enough free space to react. Using this assumption, one can estimate that the number of "active" molecules in the crystalline *trans*-stilbene is about 2%.

3.3. Photochemistry of Adduct-1

Photochemical properties of MOF-1 and Adduct-1 were studied using the samples prepared by dispersing of the targeted substances in KBr pellets. MOF-1 exhibits its own luminescence (curve 2 in Fig. 8) with the maximum at 422 nm [19]. The spectrum of MOF-1 emission is partially superimposed with that of *trans*-stilbene (curve 1 in Fig. 8). The emission spectrum of the Adduct-1 (curve 3 in Fig. 8) appears as an asymmetric band with the maximum at 405 nm and a shoulder at 390 nm. The Adduct-1 spectrum is not the sum of the spectra of MOF-1 and *trans*-stilbene, which points up the significant interaction between the frame and the guest molecules. Because the emission spectra of all the substances

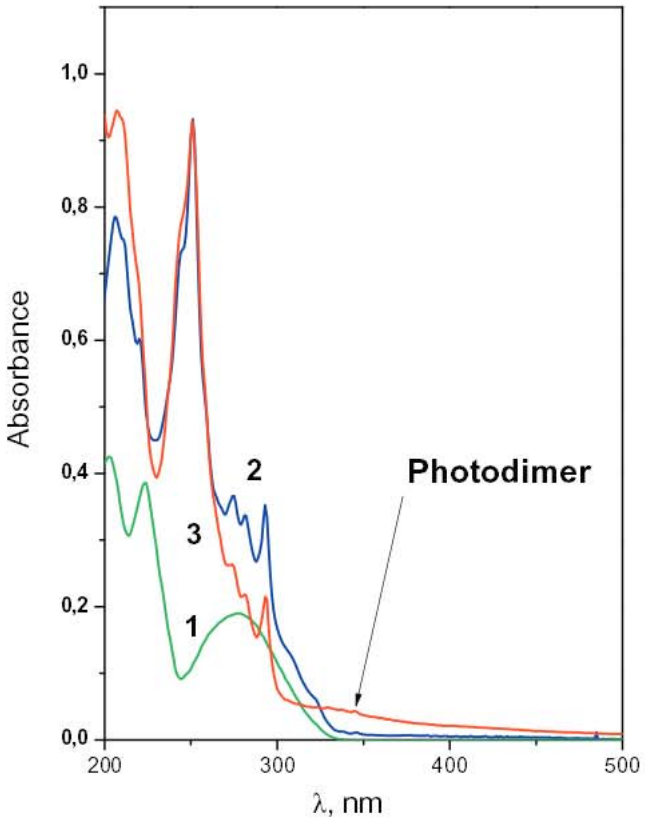

Fig. 6. UV absorbtion spectra in aqueous solutions: *cis*-stilbene (1), phenanthrene (2), and the product of the prolonged (2 hrs at 313 nm) *cis*-stilbene photolysis (3). 1 cm cell, natural content of oxygen.

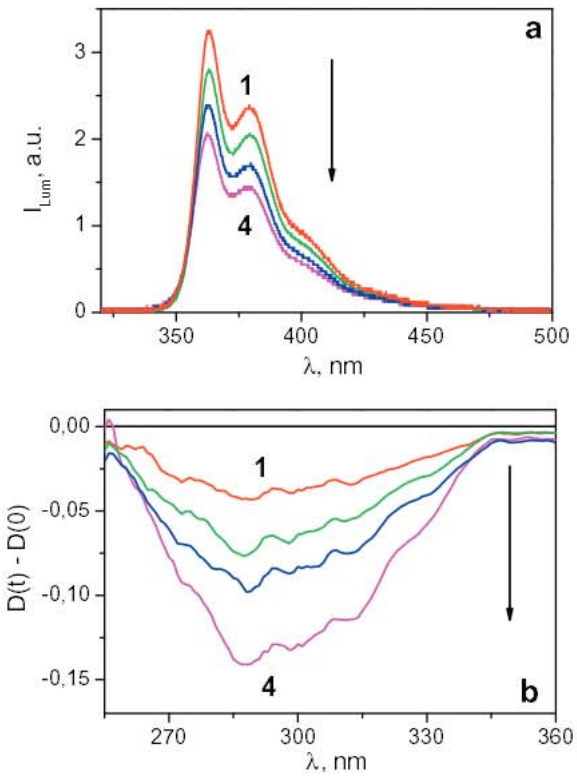

Fig. 7. Photolysis (313 nm) of *trans*-stilbene in KBr pellets. (a) Changes in the luminescence spectrum. Curves 1–4 correspond to 0, 300, 900, 2100 s of irradiation. (b) Differential changes in the UV spectrum. Curves 1–4 correspond to 20, 50, 100, 1400 s of irradiation (samples for a and b were different).

Table 1
Quantum yields (φ) of *trans–cis*-isomerization of stilbene under different conditions.

Sample	Solution in CH_3CN	KBr pellets	PS2 porous glasses	Adduct-1
φ	0.5[b]	0.008	0.2	0.2
D_{pore}[a], nm			7	1
% of reactive molecules	100	2	40	40

[a] D_{pore} is an average pore diameter for porous structures.
[b] The value taken from [30].

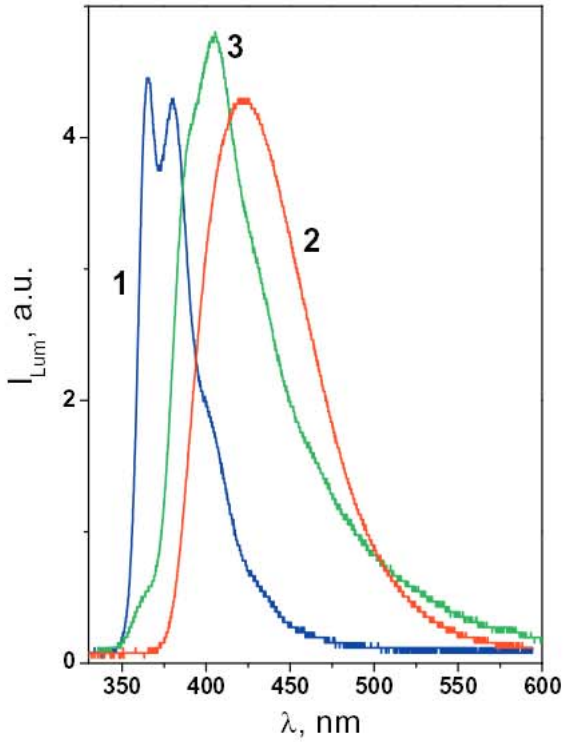

Fig. 8. Luminescence spectra of *trans*-stilbene (1), MOF-1 (2) and Adduct-1 (3) in KBr pellets.

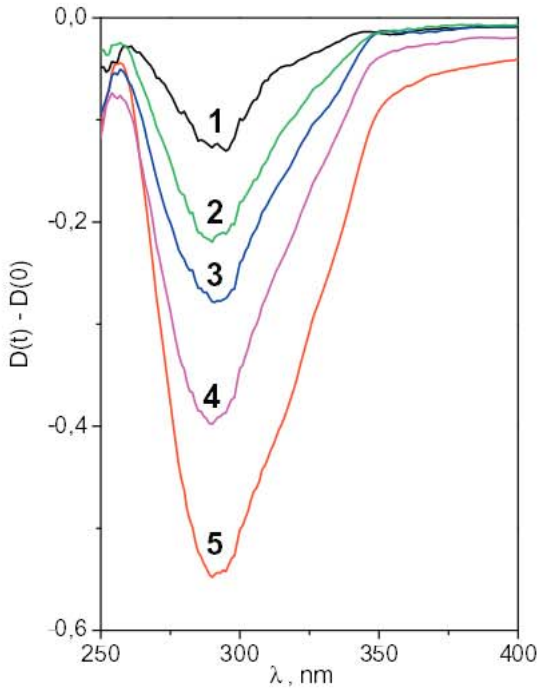

Fig. 9. Differential changes in the UV spectrum caused by irradiation (313 nm) of Adduct-1. Curves 1–5 correspond to 5, 10, 40, 100, 700 s of irradiation.

are superimposed, the monitoring of a photochemical reaction using luminescence spectroscopy seems not possible. The photochemical reaction of MOF-1 was monitored by means of UV spectroscopy.

MOF-1 was not changed under the prolonged irradiation, while Adduct-1 was found to be photochemically active. Changes in the UV spectra of KBr pellets with the dispersed Adduct-1 in the course of irradiation are shown in Fig. 9. As in the case of crystalline *trans*-stilbene photolysis (Fig. 7), only a decrease of the absorbance in the region 260–340 nm was observed. It was interpreted as *trans–cis* isomerization of stilbene incorporated to the structure of adduct. As a result, the equilibrium between *trans*- and *cis*-isomers under the irradiation is established. No evidences of the further reactions (either *cis*-stilbene photocyclization or *trans*-stilbene photodimerization, see Scheme 1) were found.

It in interesting to compare the photochemical behavior of stilbene incorporated to the MOF cage (this work), in crystalline γ-cyclodextrin inclusion complexes [22], and in para-hexanoylcalix [4] arene nanocapsules [23]. *Trans*-stilbene forming inclusion complexes with γ-cyclodextrin was observed to exhibit photodimerization (Scheme 1) [22]. Both photocyclization of *cis*-stilbene followed by phenanthrene formation and photodimerization of *trans*-stilbene (Scheme 1) were observed in para-hexanoylcalix[4]arene nanocapsules [23]. In both cases, photostationary state between *trans*- and *cis*-stilbene was established very fast (in several minutes), and the secondary reactions were the results of prolonged irradiation (2–24 h). Therefore, the quantum yields of the formation of products 4–6 (Scheme 1) were rather low. In our case, the experiments on the prolonged irradiation (several hours) were not possible because of progressive damage of KBr pellets.

The quantum yield of *trans–cis* isomerization of stilbene incorporated to Adduct-1 was estimated at the initial stage of photolysis by the value of 0.2. This is a significant value, which is an order of magnitude higher than for crystalline *trans*-stilbene (Table 1). For comparison, the experiment on the photolysis of *trans*-stilbene impregnated to the porous glass PS-2 with the average diameter of pores ca. 7 nm was performed. The results are shown in Fig. 10. As in the case of crystalline *trans*-stilbene and Adduct-1, a decrease in the stilbene band absorbance was observed and interpreted as the manifestation of *trans–cis* photoisomerization. The quantum yield of *trans*- to *cis*-transition was estimated by the value of 0.2, like in the case of Adduct-1.

The quantum yields of stilbene *trans–cis* photoisomerization (Table 1) decrease in a row:

(Solvent) > (Porous glass) ~ (Adduct with MOF) > (Crystalline state).

As it was mentioned previously, photoisomerization of stilbene needs a sufficient free volume. That is why the lowest quantum yield is observed in the case of crystalline samples, for which only surface reactions seems to be possible. In the cases of Adduct-1 and

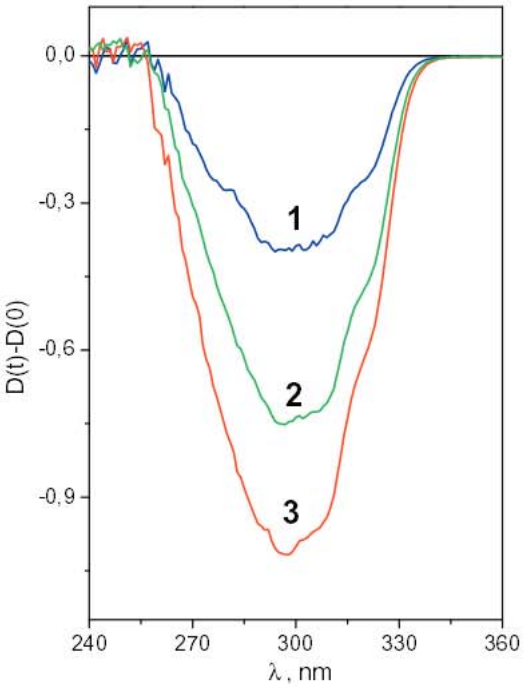

Fig. 10. Differential changes in the UV spectrum caused by irradiation (313 nm) of *trans*-stilbene in porous glass PS-2. Curves 1–5 correspond to 5, 10, 40, 100, 700 s of irradiation.

porous glasses we have a 2.5-fold drop of quantum yield in comparison with the solvent. To explain this drop, we can offer two tentative assumptions.

The first possible reason is geometrical. One can assume that the drop in quantum yield is due to impossibility for all the light-excited molecules of *trans*-stilbene to reach the 90° twisted intermediate state. Based on this assumption, one can estimate that ca. 40% of stilbene molecules incorporated either to the porous glass or to the MOF cage are "active". In the case of porous glass, the average pore diameter is large enough (7 nm [24], while the geometrical size of the plane *trans*-stilbene molecule is ca. 11 × 5 Å). Nevertheless, the structure of porous glass is not regular. Because of this, certain of the *trans*-stilbene molecules embedded to the pores can occupy positions which probably are not favorable for the formation of the twisted state. In the case of Adduct-1, the structure of the compound is regular (Fig. 3). In this case, one can propose that only the molecule of *trans*-stilbene which is situated between two others has a favorable possibility for isomerization.

The second possible reason of the quantum yield drop seems to be the interaction between the guest and host molecules, which can change the rates of different photophysical processes (e.g., speeds up the internal conversion).

4. Conclusion

In this work, supramolecular adduct of *trans*-stilbene and a metal-organic framework was synthesized. Stilbene was used as a cheap, readily available and well-studied substance for preliminary experiments. The synthesized adduct was found to demonstrate significant photochemical activity. Quantum yield of stilbene *trans–cis* isomerization in the adduct is of the same order of magnitude as in solution and much higher than for the crystalline *trans*-stilbene. We believe that the results demonstrate the perspectivity of the chosen approach to create hybrid photochromic materials. The next step will be the creation of MOF adducts with another organic photochroms characterized by high colorability and stability of the photoinduced form.

Acknowledgement

The work was supported by the Russian Foundation of Basic Research (Grant Nos. 11-03-00268 and 11-03-92605-RS).

Appendix A. Supplementary material

CCDC 950294 contains the supplementary crystallographic data for Adduct 1. These data can be obtained free of charge from The Cambridge Crystallographic Data Centre via www.ccdc.cam.ac.uk/data_request/cif. Supplementary data associated with this article can be found, in the online version, at http://dx.doi.org/10.1016/j.ica.2013.09.048.

References

[1] J.C. Crano, R.J. Guglielmetti, Organic Photochromic and Thermochromic Compounds, vol. 1, Plenum Press, NY and London, 1999. p. 2.
[2] M.V. Alfimov, O.A. Fedorova, S.P.J. Gromov, J. Photochem. Photobiol. A 158 (2003) 183.
[3] E. Hadjoudis, I.M. Mavridis, Chem. Soc. Rev. 33 (2004) 579.
[4] K. Amimoto, T. Kawato, J. Photochem. Photobiol. C 6 (2005) 207.
[5] S. Kobatake, Y. Tamada, K. Uchida, N. Kato, M. Irie, J. Am. Chem. Soc. 121 (1999) 2380.
[6] M. Morimoto, S. Kobatake, M. Irie, J. Am. Chem. Soc. 125 (2003) 11080.
[7] J. Harada, H. Uekusa, Y. Ohashi, J. Am. Chem. Soc. 121 (1999) 5809.
[8] Yu.N. Semenov, V.A. Smirnov, S.M. Aldoshin, B.G. Rogachev, Russ. Chem. Bull. 50 (2001) 2471.
[9] S. Kobatake, M. Irie, Chem. Lett. 33 (2004) 904.
[10] Hobley, V. Malatesta, R. Millini, W. Giroldini, L. Wis, M. Goto, M. Kishimoto, H. Fukumura, Chem. Commun. 14 (2000) 1339.
[11] (a) S. Benard, P. Yu, Adv. Mater. 12 (2000) 48;
(b) S. Benard, E. Riviere, P. Yu, K. Nakatani, J.F. Delouis, Chem. Mater. 13 (2001) 159;
(c) O. Godsi, U. Peskin, M. Kapon, E. Natan, Y. Eichen, Chem. Commun. 20 (2001) 2132;
(d) S.M. Aldoshin, L.A. Nikonova, V.A. Smirnov, G.V. Shilov, N.K. Nagaeva, Russ. Chem. Bull. 55 (2005) 2113.
[12] (a) S. Benard, P. Yu, Chem. Commun. 1 (2000) 65;
(b) D.G. Patel, J.B. Benedict, R.A. Kopelman, N.L. Frank, Chem. Commun. 17 (2005) 2208;
(c) M.R. di Nunzio, P.L. Gentili, A. Romani, G. Favaro, J. Phys. Chem. C 114 (2010) 6123;
(d) V.F. Plyusnin, E.M. Glebov, V.P. Grivin, V.V. Korolev, A.V. Metelitsa, N.A. Voloshin, V.I. Minkin, Russ. Chem. Bull. 60 (2011) 124.
[13] M.I. Nikolaeva, V.V. Korolev, E.A. Pritchina, E.M. Glebov, V.F. Plyusnin, A.V. Metelitsa, N.A. Voloshin, V.I. Minkin, J. Phys. Org. Chem. 24 (2011) 833.
[14] R. Pardo, M. Zayat, D. Levy, Chem. Soc. Rev. 40 (2011) 672.
[15] M.-S. Wang, G. Xu, Z.-J. Zhang, G.-C. Guo, Chem. Commun. 46 (2010) 361.
[16] T. He, J. Yao, Prog. Mater Sci. 51 (2006) 810.
[17] (a) A. Bousseksou, G. Milnar, P. Demont, J. Menegotto, J. Mater. Chem. 13 (2003) 2069;
(b) Y. Huang, Q. Pan, X.W. Dong, Z.X. Cheng, Mater. Chem. Phys. 97 (2006) 431.
[18] (a) S. Kitagawa, R. Kitaura, S.I. Noro, Angew. Chem., Int. Ed. 43 (2004) 2334;
(b) R.E. Morris, P.S. Wheatly, Angew. Chem., Int. Ed. 47 (2008) 4966;
(c) M.P. Yutkin, D.N. Dybtsev, V.P. Fedin, Russ. Chem. Rev. 80 (2011) 1009.
[19] S.A. Sapchenko, D.G. Samsonenko, D.N. Dybtsev, M.S. Melgunov, V.P. Fedin, Dalton Trans. 40 (2011) 2196.
[20] C.-S. Tsai, J.-K. Wang, R.T. Skodje, J.-C. Lin, J. Am. Chem. Soc. 127 (2005) 10788.
[21] (a) F. Gessner, A. Olea, J.H. Lobaugh, L.J. Johnston, J.C. Scaiano, J. Org. Chem. 54 (1989) 259;
(b) F. Gessner, J.C. Scaiano, J. Photochem. Photobiol. A: Chem. 67 (1992) 91.
[22] K.S.S.P. Rao, S.M. Hubig, J.N. Moorthy, J.K. Kochi, J. Org. Chem. 64 (1999) 8098.
[23] G.S. Ananchenko, K.A. Udachin, J.A. Ripmeester, T. Perrier, A.W. Coleman, Chem. Eur. J. 12 (2006) 2441.
[24] http://ns1.npkgoi.ru/r_1251/developments/opt_materials/p_glass.htm.
[25] M.S. Syamala, V. Ramamurthy, J. Org. Chem. 51 (1986) 3712.
[26] Bruker Advanced X-ray Solutions, Bruker AXS Inc., Madison, WI, 2004.
[27] G.M. Sheldrick, Acta Crystallogr. A 64 (2008) 112.
[28] H. Meier, Angew. Chem., Int. Ed. Engl. 31 (1992) 1399.
[29] (a) F.B. Mallory, C.S. Wood, J.T. Gordon, L.L. Lindquist, M.L. Savitz, J. Am. Chem. Soc. 84 (1962) 4361;
(b) F.B. Mallory, J.T. Gordon, C.S. Wood, J. Am. Chem. Soc. 85 (1963) 828;
(c) F.B. Mallory, C.S. Wood, J.T. Gordon, J. Am. Chem. Soc. 86 (1964) 3094;
(d) W.M. Moore, D.D. Morgan, F.R. Stermitz, J. Am. Chem. Soc. 85 (1963) 830;
(e) R.M. Hohstrasser, Pure Appl. Chem. 52 (1980) 2682.
[30] D.H. Waldeck, Chem. Rev. 91 (1991) 415.
[31] (a) J. Saltiel, J. Am. Chem. Soc. 89 (1967) 1036;
(b) J. Saltiel, J. Am. Chem. Soc. 90 (1968) 6394;
(c) M. Lee, G.R. Holtom, R.M. Hohstrasser, Chem. Phys. Lett. 118 (1985) 359;
(d) S. Abrash, S. Repinec, R.M. Hohstrasser, J. Chem. Phys. 93 (1990) 1041.